Geophysical Research Letters

RESEARCH LETTER
10.1029/2024GL109520

Ozone Pollution in China Affected by Climate Change in a Carbon Neutral Future as Predicted by a Process-Based Interpretable Machine Learning Method

Huimin Li[1,2], Yang Yang[1], Hang Su[2,3], Hailong Wang[4], Pinya Wang[1], and Hong Liao[1]

[1]Joint International Research Laboratory of Climate and Environment Change (ILCEC), Jiangsu Key Laboratory of Atmospheric Environment Monitoring and Pollution Control, Jiangsu Collaborative Innovation Center of Atmospheric Environment and Equipment Technology, School of Environmental Science and Engineering, Nanjing University of Information Science and Technology, Nanjing, China, [2]Multiphase Chemistry Department, Max Planck Institute for Chemistry, Mainz, Germany, [3]Institute of Atmospheric Physics, Chinese Academy of Sciences, Beijing, China, [4]Atmospheric, Climate, and Earth Sciences Division, Pacific Northwest National Laboratory, Richland, WA, USA

Abstract Ozone (O_3) pollution is a severe air quality issue in China, posing a threat to human health and ecosystems. The climate change will affect O_3 levels by directly changing physical and chemical processes of O_3 and indirectly changing natural emissions of O_3 precursors. In this study, near-surface O_3 concentrations in China in 2030 and 2060 are predicted using the process-based interpretable Extreme Gradient Boosting (XGBoost) model integrated with multi-source data. The results show that the climate-driven O_3 levels over eastern China are projected to decrease by more than 0.4 ppb in 2060 under the carbon neutral scenario (SSP1-1.9) compared with the high emission scenario (SSP5-8.5). Among this reduction, 80% is attributed to the changes in physical and chemical processes of O_3 related to a cooler climate, while the remaining 20% is attributed to the reduced biogenic isoprene emissions.

Plain Language Summary O_3 pollution is a severe air quality issue in China that threatens human health and ecosystem. Under the background of climate change, O_3 pollution will continue to evolve in the future. Here, we predict near-surface O_3 concentrations in China in 2030 and 2060 based on an interpretable machine learning method, integrated with physical and chemical processes of O_3, natural emissions of O_3 precursors, and other multi-source data. The direct (via changing physical and chemical processes of O_3) and indirect (via changing natural emissions of O_3 precursors) impacts of future climate change on O_3 concentrations are quantitatively analyzed. It demonstrates that the climate-driven O_3 levels are projected to decrease by more than 0.4 ppb in 2060 over eastern China under a carbon neutral scenario relative to a high emission scenario. The changes in physical and chemical processes under climate change play a more important role in regulating O_3 concentrations in the future than the changes in natural emissions.

Key Points:

- Climate change influences O_3 pollution in China through changing physical and chemical processes and natural precursor emissions of O_3
- Physical and chemical processes play a dominant role in regulating future near-surface O_3 concentrations over eastern China
- Carbon neutral scenario is an ideal pathway for China to mitigate both climate change and O_3 pollution in 2060

Supporting Information:

Supporting Information may be found in the online version of this article.

Correspondence to:

Y. Yang,
yang.yang@nuist.edu.cn

Citation:

Li, H., Yang, Y., Su, H., Wang, H., Wang, P., & Liao, H. (2024). Ozone pollution in China affected by climate change in a carbon neutral future as predicted by a process-based interpretable machine learning method. *Geophysical Research Letters*, *51*, e2024GL109520. https://doi.org/10.1029/2024GL109520

Received 10 APR 2024
Accepted 25 JUN 2024

Author Contributions:

Conceptualization: Huimin Li, Yang Yang
Data curation: Huimin Li
Formal analysis: Huimin Li, Yang Yang, Hang Su, Hailong Wang
Investigation: Huimin Li
Methodology: Huimin Li
Project administration: Yang Yang
Software: Huimin Li
Supervision: Yang Yang
Visualization: Huimin Li
Writing – original draft: Huimin Li
Writing – review & editing: Yang Yang, Hang Su, Hailong Wang, Pinya Wang, Hong Liao

1. Introduction

Tropospheric O_3 is generated by sunlight-driven photochemical reactions of nitrogen oxides ($NO_x \equiv NO + NO_2$) and reactive carbon species, including carbon monoxide (CO) and volatile organic compounds (VOCs). O_3 absorbs ultraviolet solar radiation and consequently acts as an important anthropogenic greenhouse gas (Checa-Garcia et al., 2018; Gao et al., 2022; Gaudel et al., 2018). Exposure to high concentrations of O_3 harms human health (Anenberg et al., 2010; Bell et al., 2004; Lelieveld et al., 2015; Malley et al., 2017), and ecosystems (Ainsworth et al., 2012; Mills et al., 2018; Monks et al., 2015; Yue et al., 2017). In recent years, although a series of emission control policies have been implemented since 2010s, China still suffers from serve O_3 pollution (Lu et al., 2020; Ni et al., 2023).

In addition to precursor emissions, recent evidences have pointed out that variations in meteorological parameters due to climate change also play vital roles in influencing O_3 concentrations (Doherty et al., 2013; Fu & Tian, 2019; Gong & Liao, 2019; Jacob & Winner, 2009; Kavassalis & Murphy, 2017; H. Li et al., 2023; M. Li et al., 2023; Lu, Zhang, Chen, et al., 2019; Lu, Zhang, & Shen, 2019; P. Wang et al., 2022; Yang et al., 2014, 2022; Zhou et al., 2022). Several studies have estimated future O_3 changes in China under different scenarios. Chen et al. (2018) projected a 10.7% increase in annual average O_3 concentrations in China by 2055 compared to 2015, due to climate warming under the RCP (Representative Concentration Pathway) 8.5 scenario through the GFDL-

CM3 climate model simulations together with a statistical downscaling approach. Based on multi-model simulations from the Coupled Model Intercomparison Project Phase 6 (CMIP6), P. Wang et al. (2022) revealed that, owing to the high sensitivity of O_3 concentrations to climate warming, extreme O_3 pollution events over North China Plain are projected to co-occur more frequently with extreme high temperatures in 2050. Zhou et al. (2022) predicted an increase in future O_3 levels over China associated with changes in Asian summer monsoon strength calculated from the CMIP6 projections under strong warming scenarios. H. Li et al. (2023) predicted a strong O_3-climate penalty over eastern China and suggested that the future climate change would expand the summertime O_3 pollution from northern China to southern China and extend it into the cold season. To mitigate risks associated with climate change, the Chinese government has committed to reach peak carbon emissions before 2030 and achieve carbon neutrality by 2060. China's net-zero climate mitigation policy can exert positive impacts on air quality, public health, and social economy (M. Li et al., 2019; Y. Wang et al., 2022). However, limited studies have investigated the impacts of climate change on O_3 pollution in China following the carbon neutral pathway.

In addition to directly interfering with the photochemical production, regional transport, and deposition of O_3, variations in meteorological conditions under climate change also indirectly affect O_3 by altering the natural precursor emissions (Fiore et al., 2015; Hong et al., 2019; Zanis et al., 2022). As one of the dominant O_3 precursors, VOCs mainly originate from terrestrial ecosystems (Kesselmeier & Staudt, 1999) and up to 90% of VOCs derive from biogenic sources (Guenther et al., 1995). Biogenic VOCs (BVOCs) emissions strongly depend on the meteorological conditions, such as ambient temperature, solar radiation, relative humidity, and precipitation (Debevec et al., 2018; Yáñez-Serrano et al., 2020; Zhang et al., 2008). S. Liu et al. (2019) showed that rising temperature enhances BVOCs emissions, which would further lead to a 0.9% increase in O_3 generation over eastern China by 2050s under the RCP8.5 scenario relative to 2015s, according to simulations conducted with the Community Multi-scale Air Quality (CMAQ) model. However, few studies have distinguished the relative importance between the direct (via changing physical and chemical processes of O_3) and indirect (via changing natural emissions of O_3 precursors) impacts of future climate change on O_3 variations in China, which is conducive to the control of O_3 pollution in the future.

Recently, machine learning (ML) methods, for example, random forest (H. Li et al., 2023; Wei et al., 2022), extreme gradient boosting (XGBoost; S. Liu et al., 2020; Yin et al., 2021), neural network (Di et al., 2017; M. Wang et al., 2024), and ensemble learning (X. Liu et al., 2022; Requia et al., 2020) have been widely adapted to estimate O_3 concentrations. ML has the advantages of computational efficiency, extraordinary performance, and high spatiotemporal resolution, which could be a practical supplement to traditional chemical transport models (CTMs). However, many ML approaches are essentially considered as black boxes, possessing inherent defects including low interpretability and lack of physicochemical mechanisms (Gilpin et al., 2018).

In this study, impacts of future climate changes on O_3 levels across China in 2030 (average of 2025–2034) and 2060 (average of 2055–2064) under both the carbon neutral scenario (SSP1-1.9) and high emission scenario (SSP5-8.5) are predicted using a ML method together with global 3-D CTM (GEOS-Chem) simulations and CMIP6 future climate projections. The individual roles of changing physical and chemical processes of O_3 and changing natural emissions of O_3 precursor (isoprene) under climate change are separately quantified. Most previous studies estimated O_3 concentrations directly through ML models, lacking physical and chemical significance. In this study, unlike traditional "black box", the interpretability and understanding of the ML model regarding physicochemical mechanisms of O_3 are creatively enhanced by adding an additional procedure during the model training and prediction phases, which incorporates the outputs of physical and chemical processes from GEOS-Chem.

2. Materials and Methods

2.1. GEOS-Chem Model Simulations

The goal of this study is to predict future climate-driven O_3 concentrations in China based on ML algorithm with the consideration of physicochemical mechanisms (Figure 1). Near-surface O_3 concentrations and the related physical and chemical process outputs for 2000–2019 simulated by the nested version of GEOS-Chem model v13.4.1 are used to train and evaluate the ML model (see Text S1 in Supporting Information S1).

Anthropogenic emissions of O_3 precursors, including non-methane VOCs (NMVOCs), NO_x and CO from 2000 to 2019 are adopted from the Community Emissions Data System version 2021_04_21 (CEDS v2021_04_21;

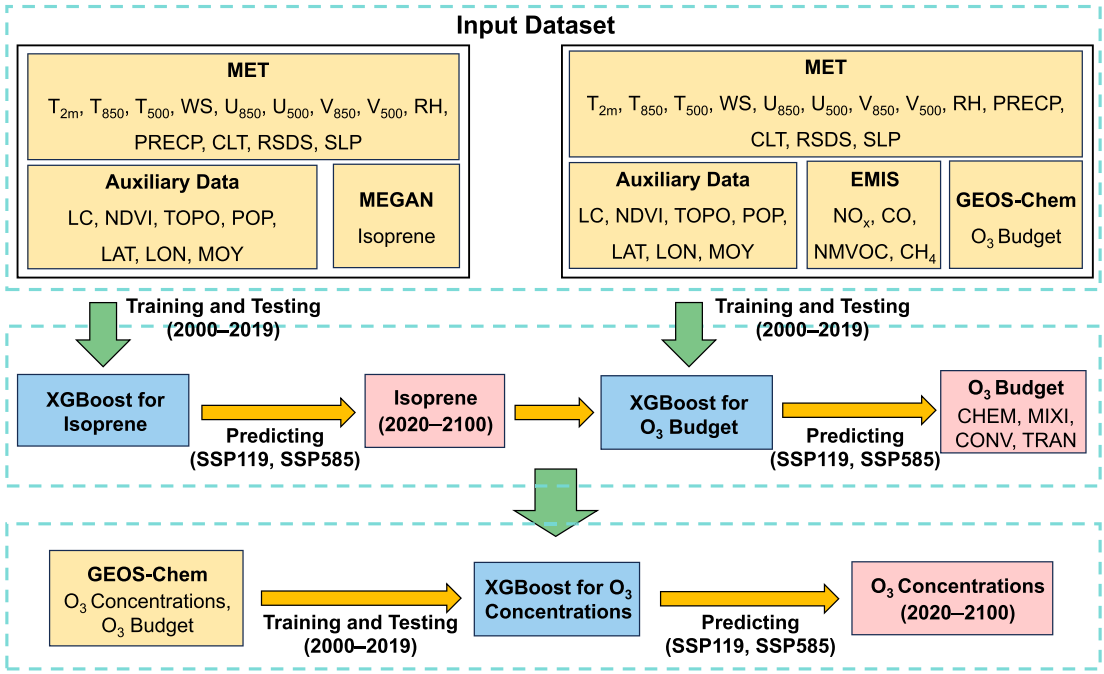

Figure 1. Flow diagram of predicting future biogenic isoprene emissions and near-surface O_3 concentrations under climate change using the Extreme Gradient Boosting (XGBoost) model.

O'Rourke et al., 2021), which provides country-level emissions that fully take into account China's efforts in mitigating air pollution since 2010s. Biogenic emissions of NMVOCs are calculated online using the Model of Emissions of Gases and Aerosols from Nature version 2.1 (MEGAN2.1; Guenther et al., 2012). The biomass burning emissions are obtained from the Global Fire Emissions Database version 4 (GFED4; van der Werf et al., 2017). Natural NO_x emissions from soil sources are estimated online with an updated version of the Berkeley–Dalhousie Soil NO_x Parameterization scheme proposed by Hudman et al. (2012). NO_x emissions produced by lightning are computed online following the algorithm described by Ott et al. (2010) and Murray et al. (2012). The methane (CH_4) mixing ratios are prescribed based on spatially interpolated monthly average surface CH_4 observations from the National Oceanic and Atmospheric Administration (NOAA) Global Monitoring Division (GMD) (Murray, 2016).

2.2. Physical and Chemical Processes of O_3

The integrated process rate analysis scheme has been fully embedded in GEOS-Chem model to identify influential physical and chemical processes that significantly affect air pollutants (Gong & Liao, 2019; Lou et al., 2015; Mu & Liao, 2014; Zhou et al., 2022), which has been widely employed to assess the relative contribution of each process to O_3 formation (Gao et al., 2016; L. Li et al., 2012; Yang et al., 2022). The process-level contributions are calculated as the differences of O_3 concentrations in each model grid cell before and after the update of corresponding physical and chemical processes. The process rates integrated within the planetary boundary layer archived from the GEOS-Chem model are used to train the ML model, which can improve the interpretability of the physicochemical mechanisms represented in the ML model. In this work, we focus on four principal processes affecting O_3 concentrations in China, including net chemical production (CHEM), horizontal advection (TRAN), vertical convection (CONV), and dry deposition and diffusion (MIXI) in the planetary boundary layer. Note that wet deposition is not considered in this study due to its small contribution to the O_3 budget (Liao et al., 2006).

2.3. CMIP6 Multi-Model Climate Projections

Future climate projections under both the carbon neutral scenario and high emission scenario that drive the O_3 projections in the ML model are obtained from CMIP6. The CMIP6 repository contains multi-model climate

projections for various Shared Socioeconomic Pathways (SSPs) based on alternative scenarios of future emissions and land use changes (O'Neill et al., 2016). The SSP1-1.9 scenario is a sustainable development pathway to keep the global warming below 1.5°C threshold, which has been widely adopted as the carbon neutral scenario (Sun et al., 2021; P. Wang et al., 2023; Zhang & Chen, 2022). In addition, the SSP5-8.5 scenario, representing the high emission pathway, is used to compare with the SSP1-1.9 results over identical future periods.

We select 8 CMIP6 global climate models (CanESM5, EC-Earth3-Veg, FGOALS-g3, GFDL-ESM4, IPSL-CM6A-LR, MIROC6, MPI-ESM1-2-LR, and MRI-ESM2-0), in which key meteorological parameters for predicting near-surface O_3 such as air temperature (2 m, 850 hPa, and 500 hPa), wind fields (850 hPa and 500 hPa), near-surface wind speed, near-surface relative humidity, precipitation rate, total cloud cover, incoming shortwave radiation at the surface, and sea level pressure for both SSP1-1.9 and SSP5-8.5 scenarios are provided. In order to minimize the inconsistencies of initial conditions in CMIP6 models and reanalysis data, the meteorological fields under future climate in CMIP6 are adjusted by the difference between CMIP6 historical meteorological variables and MERRA-2 reanalysis over 2000–2019 following H. Li et al. (2022, 2023).

2.4. Machine Learning Model Prediction

XGBoost is a supervised boosting algorithm that reduces the risk of over-fitting, captures the nonlinear relationships among predictor variables, and solves numerous data science problems in a rapid and accurate way (Chen & Guestrin, 2016). It has demonstrated high performance in O_3 studies over China (R. Li et al., 2020; R. Liu et al., 2020). As compared to other bagging tree models like random forest, XGBoost can handle more complex data while consuming fewer computing resources. It also provides greater interpretability and computational efficiency than neural networks (Hu et al., 2017). Furthermore, it is less computationally expensive compared to the CTMs, making it applicable for predicting future O_3 in this study. Considering the autocorrelation between O_3 and covariates changes over space and time series, spatiotemporal information is also added in the XGBoost model, including month of the year (MOY), and longitude (LON) and latitude (LAT) over the China domain.

Isoprene emitted by plants accounts for approximately 50% of total BVOCs and exhibits the largest potential for O_3 formation (Guenther et al., 2012). Thus, the XGBoost model is firstly constructed to predict future biogenic isoprene emissions, which are further utilized in the ML model for predicting future O_3 budget. The XGBoost model for isoprene in this study is trained with biogenic isoprene emissions from the MEGAN2.1 in GEOS-Chem, MERRA-2 meteorological data, land cover (LC), normalized difference vegetation index (NDVI), topography (TOPO), and population density (POP), LAT, LON, and MOY over 2000–2017, and the data over 2018–2019 are used for testing the model. The details of selected data used in this study are summarized in Table S1 in Supporting Information S1. The details of parameter tuning are provided in Text S2 in Supporting Information S1. The MEGAN is generally integrated in the global and regional models to estimate grided emissions. Calculating the future isoprene emissions within the coupled model requires high computational resources. The ML provides an alternative approach to predict isoprene emissions in addition to the traditional MEGAN model, and is applied here. This method is not only suitable for MEGAN, but also for other biosphere models with more complex processes.

Secondly, to individually construct the XGBoost model for predicting each O_3 budget (CHEM, TRAN, CONV, MIXI), we gather physical and chemical process rates of O_3 from GEOS-Chem, meteorological parameters from MERRA-2 and CMIP6, emissions and concentrations of O_3 precursors, and the auxiliary data (LC, NDVI, TOPO, POP, LAT, LON, and MOY). We select samples in 2000–2017 as training input data set and the remaining data over 2018–2019 for ML model testing. Then the CMIP6 data is used for future predictions.

Thirdly, we employ the XGBoost model trained by O_3 budget to predict monthly near-surface O_3 concentrations across China under both carbon neutral and high emission scenarios, with special focus on years 2030 and 2060, when China is expected to reach the carbon peak and carbon neutrality, respectively. To quantitatively analyze the relative impacts of the direct (changing physical and chemical processes of O_3) and indirect (changing natural emissions of O_3 precursors) impacts of future climate change on O_3 variations in China, the projections for both 2030 and 2060 are performed under the following scenario: (a) meteorological fields and biogenic isoprene emissions following the SSP1-1.9 (M1I1); (b) meteorological fields following the SSP1-1.9 and biogenic isoprene emissions following the SSP5-8.5 (M1I5); (c) meteorological fields and biogenic isoprene emissions following the SSP5-8.5 (M5I5); (d)meteorological fields following the SSP5-8.5 and biogenic isoprene emissions

following the SSP1-1.9 (M5I1). By comparing the four sets of O_3 projections, the roles of changing physical and chemical processes of O_3 (calculated as ((M1I1–M5I1) + (M1I5–M5I5))/2) and changing biogenic isoprene emissions (calculated as ((M1I1–M1I5) + (M5I1–M5I5))/2) can be relatively quantified.

To further improve the interpretability of the ML model, the feature importance of independent input variables in the XGBoost model is quantified using the Shapley Additive explanation (SHAP) approach (Lundberg & Lee, 2017). The SHAP calculates a value that represents the contribution of each feature to the model's outcome, which has been successfully applied in atmospheric environmental studies (Hou et al., 2022; Stirnberg et al., 2021).

3. Results

3.1. The Overall Performance of XGBoost Model

After training the model with data over 2000–2017, the remaining data samples in 2018–2019 are used to assess the prediction accuracy of the XGBoost model (Figure S1 in Supporting Information S1). The statistical metrics indicate that the XGBoost model is promising for predicting future O_3 levels across China under climate change (see Text S3 in Supporting Information S1). The SHAP method is applied to estimate the contribution of individual input variables to the projections of biogenic isoprene emissions, physical and chemical processes of O_3, and O_3 concentrations (Figures S2 and S3 in Supporting Information S1). Among all meteorological variables, the projections of biogenic isoprene emissions strongly depend on air temperature, exhibiting a positive relationship (Figure S2a in Supporting Information S1), which is consistent with previous studies (e.g., Singsaas & Sharkey, 1998). Moreover, the changing human population and massive deforestation would further alter land use, consequently affecting the functionality of terrestrial biosphere and showing negative impacts on biogenic isoprene emissions (Rosenkranz et al., 2015).

Temperature, O_3 precursor emissions, and solar radiation are the most important drivers that positively influence the rates of O_3 chemical production, while relative humidity is negatively correlated with O_3 chemical production (Figure S2b in Supporting Information S1), as mentioned in previous studies (e.g., Coates et al., 2016). With the increases in O_3 concentrations due to enhanced chemical production facilitated by favorable meteorological conditions, the O_3 dry deposition also increases (Figure S2c in Supporting Information S1). High surface air temperature and the associated low sea level pressure favor the convective transport of O_3 and have a positive impact on CONV (Figure S2d in Supporting Information S1). Horizontal transport is related to many factors, such as O_3 precursor emissions, temperature, solar radiation, precipitation, wind fields, and topography (Figure S2e in Supporting Information S1), which is more complex since these factors are interrelated. Among the four processes, only the chemical process positively promotes the O_3 production in the boundary layer, while other processes are negatively correlated with O_3 concentrations (Figure S3 in Supporting Information S1). This is because the rise in O_3 concentrations is linked to the enhanced chemical production, and higher O_3 levels favor more O_3 transport out of the domain in both horizontal and vertical directions, as well as more O_3 deposition.

3.2. Responses of Biogenic Isoprene Emissions to Future Climate Change

Biogenic isoprene emissions in 2060 under SSP1-1.9 are projected to increase compared to 2015 (average of 2010–2019), particularly over eastern China, with a growth rate of 0.1–2.0 g/m^2/yr (Figure S4 in Supporting Information S1). Figure 2 presents the changes in annual average ML-predicted biogenic isoprene emissions over China under the SSP1-1.9 (carbon neutral scenario) compared with SSP5-8.5 (high emission scenario) in 2030 and 2060. Under the background of achieving carbon peek by 2030, the biogenic isoprene emissions in SSP1-1.9 are projected to elevate by 0–0.5 g/m^2/yr over southern and eastern China, while reduce over western China compared to SSP5-8.5. Under the background of achieving carbon neutrality by 2060, biogenic isoprene emissions will significantly decrease across China under SSP1-1.9, compared to the SSP5-8.5 scenario, with a maximum decrease of 0.5–2.0 g/m^2/yr over southern China.

Variations in biogenic isoprene emissions are generally determined by meteorological parameters, especially temperature, as indicated by the feature contribution calculated in the SHAP analysis (Figure S2a in Supporting Information S1). The changes in meteorological parameters driving the ML model under the SSP1-1.9, compared to the SSP5-8.5, are shown in Figure S5 in Supporting Information S1. In 2030, the surface air temperature increases in eastern China and decreases in western China (Figure S5a in Supporting Information S1), leading to

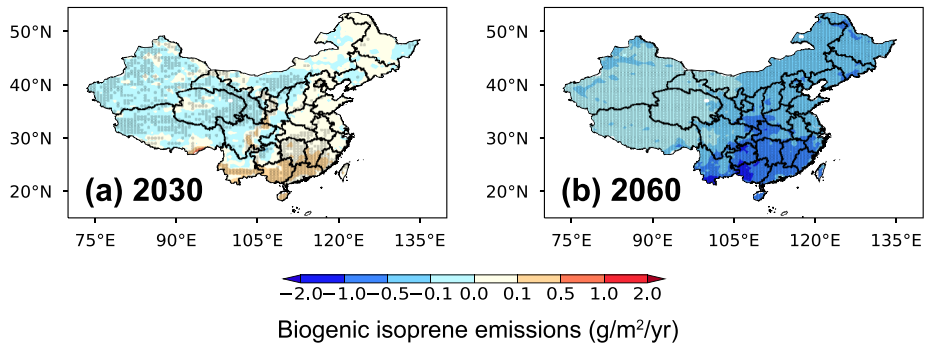

Figure 2. Spatial distributions of differences in climate-driven biogenic isoprene emissions (g/m^2/yr) between SSP1-1.9 and SSP5-8.5 scenarios (SSP1-1.9–SSP5-8.5) in (a) 2030 (average of 2025–2034) and (b) 2060 (average of 2055–2064) predicted by the ML model. The shaded areas indicate that the differences are statistically significant at the 90% confidence level.

an increase and decrease in biogenic isoprene emissions over these two respective regions. The temperature increase in eastern China mainly results from the substantial reductions in aerosols, which compensate the cooling due to the reduced greenhouse gases (P. Wang et al., 2023). In 2060, the decrease in air temperature reduces the biogenic isoprene emissions. The wet weather conditions are negatively associated with isoprene emission rates, and the increase in relative humidity over southern China in 2060 (Figure S5e in Supporting Information S1) also leads to a decrease in isoprene emissions. These results demonstrate that climate following the SSP1-1.9 scenario will be more effective than the SSP5-8.5 in reducing future biogenic isoprene emissions in 2060 when carbon neutrality is achieved in China.

3.3. Responses of Physical and Chemical Processes to Future Climate Change

Four major chemical and physical processes that contribute to the changes in O_3 concentrations over China under the carbon neutrality (SSP1-1.9), compared to the high forcing scenario (SSP5-8.5), are predicted and shown in Figure 3, including chemical production, dry deposition and diffusion, vertical convection, and horizontal advection. Among all meteorological parameters, air temperature and downward solar radiation have the most prominent influence on most processes (Figures S2b–S2e in Supporting Information S1). In 2030, facilitated by the higher temperature in eastern China and stronger solar radiation across China under SSP1-1.9, compared to SSP5-8.5 (Figures S4a and S4b in Supporting Information S1), more O_3 is produced through photochemical

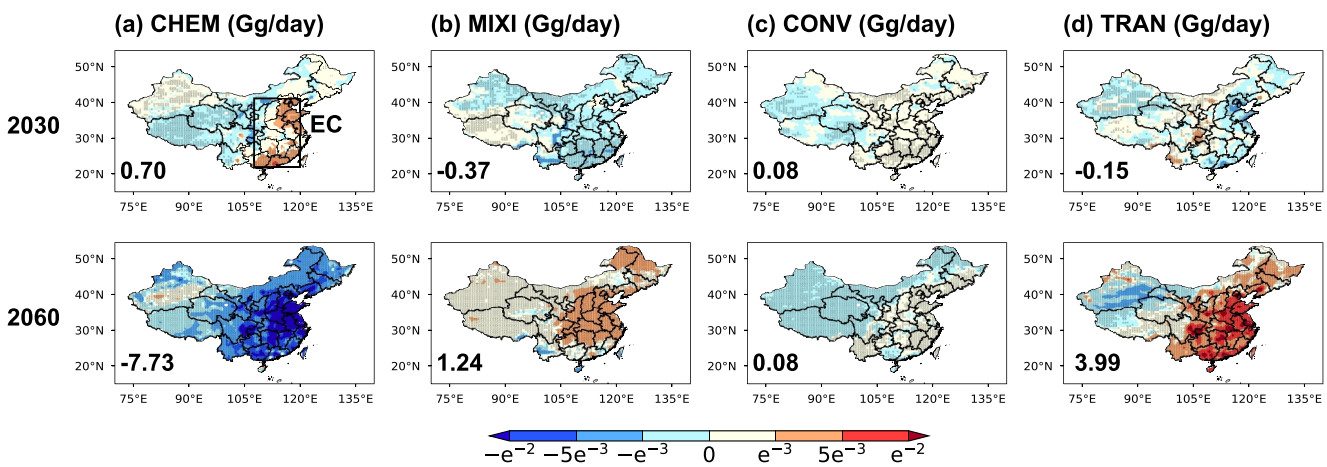

Figure 3. Spatial distributions of differences in ML-predicted physical and chemical process rates of O_3 within the boundary layer (Gg/day), including (a) net chemical production (CHEM), (b) dry deposition and diffusion (MIXI), (c) vertical convection (CONV), and (d) horizontal advection (TRAN), between SSP1-1.9 and SSP5-8.5 scenarios (SSP1-1.9–SSP5-8.5) in 2030 (average of 2025–2034, top row) and 2060 (average of 2055–2064, bottom row). The boxed area in the top panel of (a) marks eastern China (EC, 22–41°N, 107.5–120°E). The shaded areas indicate that the differences are statistically significant at the 90% confidence level. The regional average over eastern China is shown at bottom left of each panel.

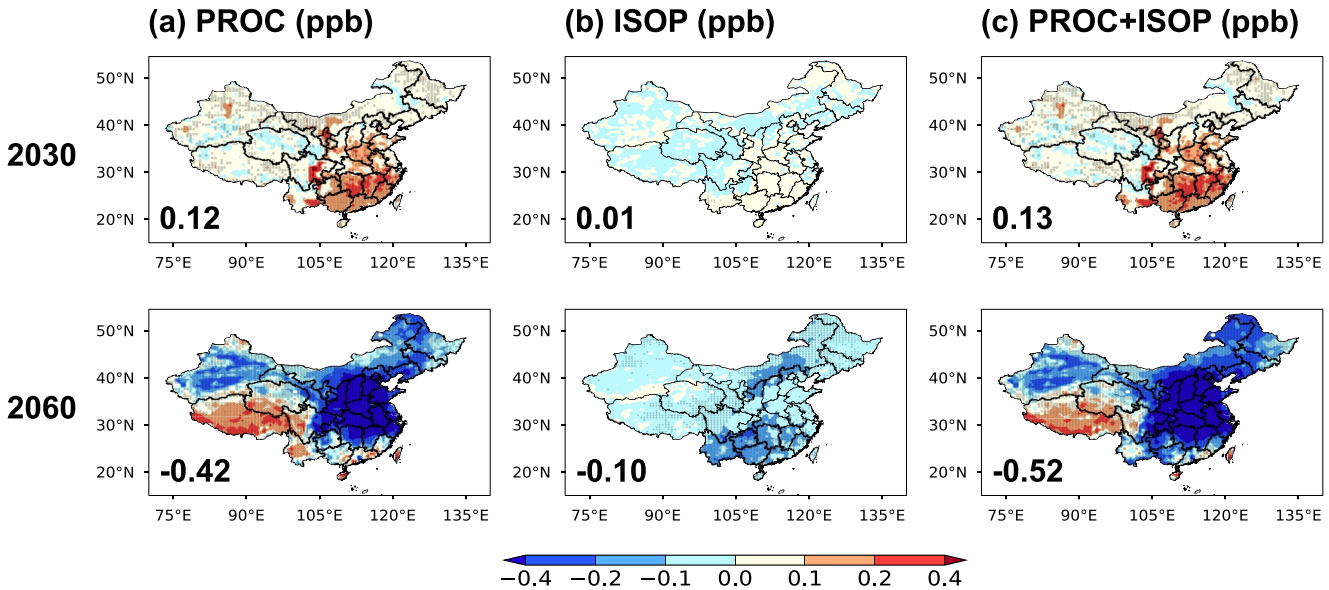

Figure 4. Spatial distributions of differences in ML-predicted near-surface O_3 concentrations (ppb) over China in response to (a) changes in physical and chemical processes of O_3 (PROC), (b) changes in biogenic isoprene emissions (ISOP), and (c) both of them (PROC + ISOP) between SSP1-1.9 and SSP5-8.5 scenarios (SSP1-1.9–SSP5-8.5) in 2030 (average of 2025–2034, top) and 2060 (average of 2055–2064, bottom). The shaded areas indicate that the differences are statistically significant at the 90% confidence level. The regional average over eastern China is shown at bottom left of each panel.

reactions (0.70 Gg day^{-1} in eastern China and hereafter), which is partially offset by the enhanced dry deposition (−0.37 Gg day^{-1}) and horizontal advection (−0.15 Gg day^{-1}) related to the increased O_3 in the analysis domain. Compared to 2015, the overall O_3 concentrations across eastern China are projected to raise mainly due to a significant increase in O_3 chemical production rate in 2060 under SSP1-1.9 scenario, followed by the increases in biogenic isoprene emissions (Figures S6 and S7 in Supporting Information S1). In 2060, associated with the lower temperature (Figure S5a in Supporting Information S1) under the SSP1-1.9, compared to SSP5-8.5 scenario, the chemical reaction rate of O_3 decreases (−7.73 Gg day^{-1}), which predominantly influences the changes in O_3 concentrations across eastern China. Furthermore, the decline in O_3 resulting from the diminished chemical production also leads to a weakened dry deposition (1.24 Gg day^{-1}) and an inflow of O_3 through horizontal advection (3.99 Gg day^{-1}) in 2060.

3.4. Responses of O_3 Concentrations in China to Future Climate Change

Figure 4 shows the predicted changes in near-surface O_3 concentrations following the SSP1-1.9 scenario compared to SSP5-8.5, due to changes in physical and chemical processes of O_3, along with biogenic isoprene emissions under climate change. In 2030, a slight temperature increase results in enhanced chemical production, causing near-surface O_3 concentrations to rise over eastern China under SSP1-1.9 compared to SSP5-8.5, with maximum increase exceeding 0.2 ppb. In 2060, O_3 concentrations decrease by more than 0.4 ppb across eastern China, which are attributed to the weakened chemical production related to the cooling climate under SSP1-1.9, as compared with SSP5-8.5. Changes in biogenic isoprene emissions only cause a small O_3 concentration change (within ±0.1 ppb) over China in 2030. The reductions in isoprene emission in 2060 induce a decline in O_3 concentrations by 0.1–0.4 ppb over southern China and 0.1–0.2 ppb over part of northern China. The changes in O_3 driven by physical and chemical processes as well as biogenic isoprene emissions are comparable to those driven by processes alone, suggesting that changes in physical and chemical processes induced by meteorological factors under climate change are the major drivers of future O_3 variations over China.

Figure 4 summarizes the variations in near-surface O_3 concentrations averaged over eastern China due to changes in physical and chemical processes of O_3, and changes in biogenic isoprene emissions. In 2030, compared with SSP5-8.5, climate change under SSP1-1.9 leads to a 0.13 ppb increase in O_3 level, more than 90% of which is attributed to changes in physical and chemical processes of O_3. In 2060, the average concentration of O_3 in eastern China is projected to decrease by 0.52 ppb following SSP1-1.9 compared to SSP5-8.5. About 80% of the O_3

reduction is due to changes in physical and chemical processes of O_3, while 20% is due to changes in biogenic isoprene emissions under climate change, suggesting that the physical and chemical processes play a more important role than natural BVOCs emissions in regulating O_3 concentrations in the future.

4. Conclusion and Discussions

In order to keep the global warming below 1.5°C threshold and reduce the risks of climate change, numerous countries around the world, including China, have committed to achieving carbon neutrality in the near future. Climate change would influence O_3 pollution in China through changing physical and chemical processes of O_3 and natural emissions of O_3 precursors. In this study, unlike the traditional "black box" ML models, an interpretable XGBoost model including physical and chemical mechanisms of O_3 production, based on multi-source data fusion and SHAP method, is established to predict future near-surface O_3 concentrations over China in 2030 and 2060 under carbon neutral scenario (SSP1-1.9) and high emission scenario (SSP5-8.5). Biogenic isoprene emissions and four physical and chemical processes (including net chemical production, horizontal advection, vertical convection, dry deposition and diffusion) that influence O_3 concentrations are firstly predicted by the XGBoost model. Subsequently, O_3 concentrations are further estimated based on these factors. The trained XGBoost model shows high accuracy with R^2 of 0.95 and MRE of 5% between simulated and predicted O_3 concentrations in China.

The isoprene emissions are typically linked to climate change, which can further affect O_3 concentrations. Warmer climate, as the primary influential factor, leads to an increase (0–0.5 $g/m^2/yr$) of biogenic isoprene emissions over eastern China in 2030 under SSP1-1.9 relative to the SSP5-8.5 scenario. With decrease of air temperature and frequent occurrence of wet weather conditions, the isoprene emission rates over eastern China in 2060 under SSP1-1.9 are projected to decrease (0.5–2 $g/m^2/yr$) compared to SSP5-8.5. The changes in biogenic isoprene emissions only cause a minor variation in O_3 concentrations (within ±0.1 ppb) over eastern China in 2030. The reductions in isoprene emissions in 2060 induce a decline in O_3 concentrations by 0.1–0.4 ppb over southern China and 0.1–0.2 ppb over part of northern China.

Due to the higher air temperature in 2030 associated with aerosol reductions, the chemical production rates of O_3 will be enhanced over eastern China. Consequently, O_3 levels are projected to rise, reaching a maximum increase over 0.2 ppb under SSP1-1.9 relative to the SSP5-8.5 scenario. In contrast, associated with lower temperature under SSP1-1.9 scenario in 2060, O_3 concentrations will dramatically decrease by more than 0.4 ppb across eastern China mainly due to the weakened chemical production. Changes in physical and chemical processes of O_3 account for the majority of future O_3 variations, explaining 80% of the O_3 reduction in 2060 under SSP1-1.9 compared to SSP5-8.5. Our results suggest that the physical and chemical processes play a more important role than natural BVOCs emissions in regulating O_3 concentrations in the future under the carbon neutral scenario.

In our study, there are several limitations associated with input data for GEOS-Chem model simulations, CMIP6 multi-model simulations, and the XGBoost model, which can result in uncertainties in O_3 projections over China. First, the performance of the trained XGBoost model highly depends on the accuracy of the GEOS-Chem model simulations, which is further related to MERRA-2 reanalysis data, emission inventories, and physicochemical parameterizations. The GEOS-Chem model shows notable systematic biases in simulating O_3 concentrations compared to observations, with an average bias of 10% over China (Lou et al., 2014), and a bias of 7.7 ppb (17.5%) across eastern China (Yin et al., 2021). GEOS-Chem model also overestimates isoprene levels at most southern sites during the growing season, but underestimates at most northern sites over China (Zhang et al., 2020). Second, meteorological variables under different scenarios from CMIP6 multi-model simulations can also induce biases (Xu et al., 2021). Third, the land use data, topography, and population density are fixed at a specific year when predicting future O_3, which will also vary with climate change and give rise to prediction biases. Moreover, the dependence and correlation among selected input features used in the ML model would exert a notable influence on the SHAP values, potentially resulting in spurious explanations (Silva & Keller, 2024). In addition, it is noteworthy that the performance of XGBoost model is unsatisfactory in predicting vertical convection of O_3, likely related to the low vertical resolution of meteorological variables adopted in the ML model (e.g., wind fields at 850 hPa and 500 hPa). Further work should fully consider the impacts of the vertical resolution of wind fields on the vertical transport and mixing of O_3 to improve the model's performance.

Conflict of Interest

The contact author has declared that neither they nor their co-authors have any competing interests.

Data Availability Statement

The projected O_3 concentrations in this study are available for download at Zenodo (Yang, 2023).

Acknowledgments
This study was supported by the National Natural Science Foundation of China (Grant 42293320), Jiangsu Science Fund for Distinguished Young Scholars (Grant BK20211541), Jiangsu Science Fund for Carbon Neutrality (Grant BK20220031), Jiangsu Innovation and Entrepreneurship Team (Grant JSSCTD202346), and the Graduate Research Innovation Project in Jiangsu province (Grant KYCX23_1380). Huimin Li is supported by the China Scholarship Council during her visit at the Max Planck Institute for Chemistry. Hailong Wang acknowledges the support by the U.S. Department of Energy (DOE), Office of Science, Office of Biological and Environmental Research (BER), as part of the Earth and Environmental System Modeling program. The Pacific Northwest National Laboratory (PNNL) is operated for DOE by the Battelle Memorial Institute under contract DE-AC05-76RLO1830.

References

Ainsworth, E. A., Yendrek, C. R., Sitch, S., Collins, W. J., & Emberson, L. D. (2012). The effects of tropospheric ozone on net primary productivity and implications for climate change. *Annual Review of Plant Biology*, *63*(1), 637–661. https://doi.org/10.1146/annurev-arplant-042110-103829

Anenberg, S. C., Horowitz, L. W., Tong, D. Q., & West, J. J. (2010). An estimate of the global burden of anthropogenic ozone and fine particulate matter on premature human mortality using atmospheric modeling. *Environmental Health Perspectives*, *118*(9), 1189–1195. https://doi.org/10.1289/ehp.0901220

Bell, M., McDermott, A., Zeger, S., Samet, J., & Dominici, F. (2004). Ozone and short-term mortality in 95 US urban communities, 1987–2000. *Journal of the American Medical Association*, *292*(19), 2372–2378. https://doi.org/10.1001/jama.292.19.2372

Checa-Garcia, R., Hegglin, M. I., Kinnison, D., Plummer, D. A., & Shine, K. P. (2018). Historical tropospheric and stratospheric ozone radiative forcing using the CMIP6 database. *Geophysical Research Letters*, *45*(7), 3264–3273. https://doi.org/10.1002/2017GL076770

Chen, K., Fiore, A. M., Chen, R., Jiang, L., Jones, B., Schneider, A., et al. (2018). Future ozone-related acute excess mortality under climate and population change scenarios in China: A modeling study. *PLoS Medicine*, *15*(7), e1002598. https://doi.org/10.1371/journal.pmed.1002598

Chen, T., & Guestrin, C. (2016). XGBoost: A scalable tree boosting system. In *Proceedings of the 22nd ACM SIGKDD international conference on knowledge discovery and data mining*. ACM.

Coates, J., Mar, K. A., Ojha, N., & Butler, T. M. (2016). The influence of temperature on ozone production under varying NO_x conditions—A modelling study. *Atmospheric Chemistry and Physics*, *16*(18), 11601–11615. https://doi.org/10.5194/acp-16-11601-2016

Debevec, C., Sauvage, S., Gros, V., Sellegri, K., Sciare, J., Pikridas, M., et al. (2018). Driving parameters of biogenic volatile organic compounds and consequences on new particle formation observed at an eastern Mediterranean background site. *Atmospheric Chemistry and Physics*, *18*(19), 14297–14325. https://doi.org/10.5194/acp-18-14297-2018

Di, Q., Rowland, S., Koutrakis, P., & Schwartz, J. (2017). A hybrid model for spatially and temporally resolved ozone exposures in the continental United States. *Journal of the Air & Waste Management Association*, *67*(1), 39–52. https://doi.org/10.1080/10962247.2016.1200159

Doherty, R. M., Wild, O., Shindell, D. T., Zeng, G., MacKenzie, I. A., Collins, W. J., et al. (2013). Impacts of climate change on surface ozone and intercontinental ozone pollution: A multi-model study. *Journal of Geophysical Research*, *118*(9), 3744–3763. https://doi.org/10.1002/jgrd.50266

Fiore, A. M., Naik, V., & Leibensperger, E. M. (2015). Air quality and climate connections. *Journal of the Air & Waste Management Association*, *65*(6), 645–685. https://doi.org/10.1080/10962247.2015.1040526

Fu, T.-M., & Tian, H. (2019). Climate change penalty to ozone air quality: Review of current understandings and knowledge gaps. *Current Pollution Reports*, *5*(3), 159–171. https://doi.org/10.1007/s40726-019-00115-6

Gao, J., Yang, Y., Wang, H., Wang, P., Li, H., Li, M., et al. (2022). Fast climate responses to emission reductions in aerosol and ozone precursors in China during 2013–2017. *Atmospheric Chemistry and Physics*, *22*(11), 7131–7142. https://doi.org/10.5194/acp-22-7131-2022

Gao, J., Zhu, B., Xiao, H., Kang, H., Hou, X., & Shao, P. (2016). A case study of surface ozone source apportionment during a high concentration episode, under frequent shifting wind conditions over the Yangtze River Delta, China. *Science of the Total Environment*, *544*, 853–863. https://doi.org/10.1016/j.scitotenv.2015.12.039

Gaudel, A., Cooper, O. R., Ancellet, G., Barret, B., Boynard, A., Burrows, J. P., et al. (2018). Tropospheric Ozone Assessment Report: Present-day distribution and trends of tropospheric ozone relevant to climate and global atmospheric chemistry model evaluation. *Elementa: Science of the Anthropocene*, *6*, 39. https://doi.org/10.1525/elementa.291

Gilpin, L. H., Bau, D., Yuan, B. Z., Bajwa, A., Specter, M., & Kagal, L. (2018). Explaining explanations: An overview of interpretability of machine learning. In *2018 IEEE 5th international conference on data science and advanced analytics (DSAA)* (pp. 80–89). Institute of Electrical and Electronics Engineers. https://doi.org/10.1109/DSAA.2018.00018

Gong, C., & Liao, H. (2019). A typical weather pattern for ozone pollution events in North China. *Atmospheric Chemistry and Physics*, *19*(22), 13725–13740. https://doi.org/10.5194/acp-19-13725-2019

Guenther, A., Hewitt, C. N., Erickson, D., Fall, R., Geron, C., Graedel, T., et al. (1995). A global model of natural volatile organic compound emissions. *Journal of Geophysical Research*, *100*(D5), 8873–8892. https://doi.org/10.1029/94jd02950

Guenther, A. B., Jiang, X., Heald, C. L., Sakulyanontvittaya, T., Duhl, T., Emmons, L. K., & Wang, X. (2012). The model of Emissions of Gases and Aerosols from Nature version 2.1 (MEGAN2.1): An extended and updated framework for modeling biogenic emissions. *Geoscientific Model Development*, *5*(6), 1471–1492. https://doi.org/10.5194/gmd-5-1471-2012

Hong, C., Zhang, Q., Zhang, Y., Davis, S. J., Tong, D., Zheng, Y., et al. (2019). Impacts of climate change on future air quality and human health in China. *Proceedings of the National Academy of Sciences*, *116*(35), 17193–17200. https://doi.org/10.1073/pnas.1812881116

Hou, L., Dai, Q., Song, C., Liu, B., Guo, F., Dai, T., et al. (2022). Revealing drivers of haze pollution by explainable machine learning. *Environmental Science and Technology Letters*, *9*(2), 112–119. https://doi.org/10.1021/acs.estlett.1c00865

Hu, X., Belle, J. H., Meng, X., Wildani, A., Waller, L. A., Strickland, M. J., & Liu, Y. (2017). Estimating $PM_{2.5}$ concentrations in the conterminous United States using the random forest approach. *Environmental Science & Technology*, *51*(12), 6936–6944. https://doi.org/10.1021/acs.est.7b01210

Hudman, R. C., Moore, N. E., Mebust, A. K., Martin, R. V., Russell, A. R., Valin, L. C., & Cohen, R. C. (2012). Steps towards a mechanistic model of global soil nitric oxide emissions: Implementation and space based-constraints. *Atmospheric Chemistry and Physics*, *12*(16), 7779–7795. https://doi.org/10.5194/acp-12-7779-2012

Jacob, D. J., & Winner, D. A. (2009). Effect of climate change on air quality. *Atmospheric Environment*, *43*(1), 51–63. https://doi.org/10.1016/j.atmosenv.2008.09.051

Kavassalis, S. C., & Murphy, J. G. (2017). Understanding ozone-meteorology correlations: A role for dry deposition. *Geophysical Research Letters*, *44*(6), 2922–2931. https://doi.org/10.1002/2016gl071791

Kesselmeier, J., & Staudt, M. (1999). Biogenic volatile organic compounds (VOC): An overview on emission, physiology and ecology. *Journal of Atmospheric Chemistry*, *33*(1), 23–88. https://doi.org/10.1023/A:1006127516791

Lelieveld, J., Evans, J. S., Fnais, M., Giannadaki, D., & Pozzer, A. (2015). The contribution of outdoor air pollution sources to premature mortality on a global scale. *Nature*, *525*(7569), 367–371. https://doi.org/10.1038/nature15371

Li, H., Yang, Y., Jin, J., Wang, H., Li, K., Wang, P., & Liao, H. (2023). Climate-driven deterioration of future ozone pollution in Asia predicted by machine learning with multi-source data. *Atmospheric Chemistry and Physics*, *23*(2), 1131–1145. https://doi.org/10.5194/acp-23-1131-2023

Li, H., Yang, Y., Wang, H., Wang, P., Yue, X., & Liao, H. (2022). Projected aerosol changes driven by emissions and climate change using a machine learning method. *Environmental Science & Technology*, *56*(7), 3884–3893. https://doi.org/10.1021/acs.est.1c04380

Li, L., Chen, C., Huang, C., Huang, H., Zhang, G., Wang, Y., et al. (2012). Process analysis of regional ozone formation over the Yangtze River Delta, China using the community Multi-Scale Air Quality modeling system. *Atmospheric Chemistry and Physics*, *12*(22), 10971–10987. https://doi.org/10.5194/acp-12-10971-2012

Li, M., Yang, Y., Wang, H., Li, H., Wang, P., & Liao, H. (2023). Summertime ozone pollution in China affected by stratospheric quasi-biennial oscillation. *Atmospheric Chemistry and Physics*, *23*(2), 1533–1544. https://doi.org/10.5194/acp-23-1533-2023

Li, M., Zhang, D., Li, C.-T., Selin, N. E., & Karplus, V. J. (2019). Co-benefits of China's climate policy for air quality and human health in China and transboundary regions in 2030. *Environmental Research Letters*, *14*(8), 084006. https://doi.org/10.1088/1748-9326/ab26ca

Li, R., Cui, L., Fu, H., Li, J., Zhao, Y., & Chen, J. (2020). Satellite-based estimation of full-coverage ozone (O_3) concentration and health effect assessment across Hainan Island. *Journal of Cleaner Production*, *244*, 118773. https://doi.org/10.1016/j.jclepro.2019.118773

Liao, H., Chen, W.-T., & Seinfeld, J. H. (2006). Role of climate change in global predictions of future tropospheric ozone and aerosols. *Journal of Geophysical Research*, *111*(D12), D12304. https://doi.org/10.1029/2005jd006852

Liu, R., Ma, Z., Liu, Y., Shao, Y., Zhao, W., & Bi, J. (2020). Spatiotemporal distributions of surface ozone levels in China from 2005 to 2017: A machine learning approach. *Environment International*, *142*, 105823. https://doi.org/10.1016/j.envint.2020.105823

Liu, S., Xing, J., Zhang, H., Ding, D., Zhang, F., Zhao, B., et al. (2019). Climate-driven trends of biogenic volatile organic compound emissions and their impacts on summertime ozone and secondary organic aerosol in China in the 2050s. *Atmospheric Environment*, *218*, 117020. https://doi.org/10.1016/j.atmosenv.2019.117020

Liu, X., Zhu, Y., Xue, L., Desai, A. R., & Wang, H. (2022). Cluster-enhanced ensemble learning for mapping global monthly surface ozone from 2003 to 2019. *Geophysical Research Letters*, *49*(11), e2022GL097947. https://doi.org/10.1029/2022GL097947

Lou, S., Liao, H., Yang, Y., & Mu, Q. (2015). Simulation of the interannual variations of tropospheric ozone over China: Roles of variations in meteorological parameters and anthropogenic emissions. *Atmospheric Environment*, *122*, 839–851. https://doi.org/10.1016/j.atmosenv.2015.08.081

Lou, S., Liao, H., & Zhu, B. (2014). Impacts of aerosols on surface-layer ozone concentrations in China through heterogeneous reactions and changes in photolysis rates. *Atmospheric Environment*, *85*, 123–138. https://doi.org/10.1016/j.atmosenv.2013.12.004

Lu, X., Zhang, L., Chen, Y., Zhou, M., Zheng, B., Li, K., et al. (2019). Exploring 2016–2017 surface ozone pollution over China: Source contributions and meteorological influences. *Atmospheric Chemistry and Physics*, *19*(12), 8339–8361. https://doi.org/10.5194/acp-19-8339-2019

Lu, X., Zhang, L., & Shen, L. (2019). Meteorology and climate influences on tropospheric ozone: A Review of natural sources, chemistry, and transport patterns. *Current Pollution Reports*, *5*(4), 238–260. https://doi.org/10.1007/s40726-019-00118-3

Lu, X., Zhang, L., Wang, X., Gao, M., Li, K., Zhang, Y., et al. (2020). Rapid increases in warm-season surface ozone and resulting health impact in China since 2013. *Environmental Science and Technology Letters*, *7*(4), 240–247. https://doi.org/10.1021/acs.estlett.0c00171

Lundberg, S. M., & Lee, S.-I. (2017). A unified approach to interpreting model predictions. *Advances in Neural Information Processing Systems*, *30*, 4768–4777. https://doi.org/10.48550/arXiv.1705.07874

Malley, C. S., Henze, D. K., Kuylenstierna, J. C. I., Vallack, H., Davila, Y., Anenberg, S. C., et al. (2017). Updated global estimates of respiratory mortality in adults ≥ 30 Years of age attributable to long-term ozone exposure. *Environmental Health Perspectives*, *125*(8), 087021. https://doi.org/10.1289/EHP1390

Mills, G., Pleijel, H., Malley, C. S., Sinha, B., Cooper, O. R., Schultz, M. G., et al. (2018). Tropospheric ozone assessment report: Present-day tropospheric ozone distribution and trends relevant to vegetation. *Elementa: Science of the Anthropocene*, *6*, 47. https://doi.org/10.1525/elementa.302

Monks, P. S., Archibald, A. T., Colette, A., Cooper, O., Coyle, M., Derwent, R., et al. (2015). Tropospheric ozone and its precursors from the urban to the global scale from air quality to short-lived climate forcer. *Atmospheric Chemistry and Physics*, *15*, 8889–8973. https://doi.org/10.5194/acp-15-8889-2015

Mu, Q., & Liao, H. (2014). Simulation of the interannual variations of aerosols in China: Role of variations in meteorological parameters. *Atmospheric Chemistry and Physics*, *14*(18), 9597–9612. https://doi.org/10.5194/acp-14-9597-2014

Murray, L. T. (2016). Lightning NO_x and impacts on air quality. *Current Pollution Reports*, *2*, 115–133. https://doi.org/10.1007/s40726-016-0031-7

Murray, L. T., Jacob, D. J., Logan, J. A., Hudman, R. C., & Koshak, W. J. (2012). Optimized regional and interannual variability of lightning in a global chemical transport model constrained by LIS/OTD satellite data. *Journal of Geophysical Research*, *1117*(D20), D20307. https://doi.org/10.1029/2012jd017934

Ni, Y., Yang, Y., Wang, H., Li, H., Li, M., Wang, P., et al. (2023). Contrasting changes in ozone during 2019–2021 between eastern and the other regions of China attributed to anthropogenic emissions and meteorological conditions. *Science of the Total Environment*, *908*, 168272. https://doi.org/10.1016/j.scitotenv.2023.168272

O'Neill, B. C., Tebaldi, C., van Vuuren, D. P., Eyring, V., Friedlingstein, P., Hurtt, G., et al. (2016). The scenario model Intercomparison Project (ScenarioMIP) for CMIP6. *Geoscientific Model Development*, *9*, 3461–3482. https://doi.org/10.5194/gmd-9-3461-2016

O'Rourke, P., Smith, S., Mott, A., Ahsan, H., Mcduffie, E., Crippa, M., et al. (2021). CEDS v_2021_04_21 Gridded emissions data. https://doi.org/10.25584/PNNLDATAHUB/1779095

Ott, L. E., Pickering, K. E., Stenchikov, G. L., Allen, D. J., DeCaria, A. J., Ridley, B., et al. (2010). Production of lightning NO_x and its vertical distribution calculated from three-dimensional cloud-scale chemical transport model simulations. *Journal of Geophysical Research*, *115*(D4), D04301. https://doi.org/10.1029/2009JD011880

Requia, W. J., Di, Q., Silvern, R., Kelly, J. T., Koutrakis, P., Mickley, L. J., et al. (2020). An ensemble learning approach for estimating high spatiotemporal resolution of ground-level ozone in the contiguous United States. *Environmental Science & Technology*, *54*(18), 11037–11047. https://doi.org/10.1021/acs.est.0c01791

Rosenkranz, M., Pugh, T. A. M., Schnitzler, J. P., & Arneth, A. (2015). Effect of land-use change and management on biogenic volatile organic compound emissions—Selecting climate-smart cultivars. *Plant, Cell and Environment*, *38*(9), 1896–1912. https://doi.org/10.1111/pce.12453

Silva, S. J., & Keller, C. A. (2024). Limitations of XAI methods for process-level understanding in the atmospheric sciences. *Artificial Intelligence for the Earth Systems*, *3*(1), e230045. https://doi.org/10.1175/AIES-D-23-0045.1

Singsaas, E. L., & Sharkey, T. D. (1998). The regulation of isoprene emission responses to rapid leaf temperature fluctuations. *Plant, Cell and Environment*, *21*(11), 1181–1188. https://doi.org/10.1046/j.1365-3040.1998.00380.x

Stirnberg, R., Cermak, J., Kotthaus, S., Haeffelin, M., Andersen, H., Fuchs, J., et al. (2021). Meteorology-driven variability of air pollution (PM_1) revealed with explainable machine learning. *Atmospheric Chemistry and Physics*, *21*(5), 3919–3948. https://doi.org/10.5194/acp-21-3919-2021

Sun, T., Ocko, I. B., Sturcken, E., & Hamburg, S. P. (2021). Path to net zero is critical to climate outcome. *Scientific Reports*, *11*(1), 22173. https://doi.org/10.1038/s41598-021-01639-y

van der Werf, G. R., Randerson, J. T., Giglio, L., van Leeuwen, T. T., Chen, Y., Rogers, B. M., et al. (2017). Global fire emissions estimates during 1997–2016. *Earth System Science Data*, *9*(2), 697–720. https://doi.org/10.5194/essd-9-697-2017

Wang, M., Chen, X., Jiang, Z., He, T. L., Jones, D., Liu, J., & Shen, Y. (2024). Meteorological and anthropogenic drivers of surface ozone change in the North China Plain in 2015–2021. *Science of the Total Environment*, *906*, 167763. https://doi.org/10.1016/j.scitotenv.2023.167763

Wang, P., Yang, Y., Li, H., Chen, L., Dang, R., Xue, D., et al. (2022). North China Plain as a hot spot of ozone pollution exacerbated by extreme high temperatures. *Atmospheric Chemistry and Physics*, *22*(7), 4705–4719. https://doi.org/10.5194/acp-22-4705-2022

Wang, P., Yang, Y., Xue, D., Ren, L., Tang, J., Leung, L. R., & Liao, H. (2023). Aerosols overtake greenhouse gases causing a warmer climate and more weather extremes toward carbon neutrality. *Nature Communications*, *14*(1), 7257. https://doi.org/10.1038/s41467-023-42891-2

Wang, Y., Xie, M., Wu, Y., Zhang, X., Wang, M., Zhang, Y., et al. (2022). Ozone-related co-benefits of China's climate mitigation policy. *Resources, Conservation and Recycling*, *182*, 106288. https://doi.org/10.1016/j.resconrec.2022.106288

Wei, J., Li, Z., Li, K., Dickerson, R., Pinker, R., Wang, J., et al. (2022). Full-coverage mapping and spatiotemporal variations of ground-level ozone (O_3) pollution from 2013 to 2020 across China. *Remote Sensing of Environment*, *270*, 112775. https://doi.org/10.1016/j.rse.2021.112775

Xu, Z., Han, Y., Tam, C. Y., Yang, Z., & Fu, C. (2021). Bias-corrected CMIP6 global dataset for dynamical downscaling of the historical and future climate (1979–2100). *Scientific Data*, *8*(1), 293. https://doi.org/10.1038/s41597-021-01079-3

Yáñez-Serrano, A. M., Bourtsoukidis, E., Alves, E. G., Bauwens, M., Stavrakou, T., Llusià, J., et al. (2020). Amazonian biogenic volatile organic compounds under global change. *Global Change Biology*, *26*(9), 4722–4751. https://doi.org/10.1111/gcb.15185

Yang, Y. (2023). Data for "Ozone pollution in China affected by climate change in a carbon neutral future as predicted by a process-based interpretable machine learning method" [Dataset]. *Zenodo*. https://doi.org/10.5281/zenodo.10408554

Yang, Y., Li, M., Wang, H., Li, H., Wang, P., Li, K., et al. (2022). ENSO modulation of summertime tropospheric ozone over China. *Environmental Research Letters*, *17*(3), 034020. https://doi.org/10.1088/1748-9326/ac54cd

Yang, Y., Liao, H., & Li, J. (2014). Impacts of the East Asian summer monsoon on interannual variations of summertime surface-layer ozone concentrations over China. *Atmospheric Chemistry and Physics*, *14*(13), 6867–6879. https://doi.org/10.5194/acp-14-6867-2014

Yin, H., Lu, X., Sun, Y., Li, K., Gao, M., Zheng, B., & Liu, C. (2021). Unprecedented decline in summertime surface ozone over eastern China in 2020 comparably attributable to anthropogenic emission reductions and meteorology. *Environmental Research Letters*, *16*(12), 124069. https://doi.org/10.1088/1748-9326/ac3e22

Yue, X., Unger, N., Harper, K., Xia, X., Liao, H., Zhu, T., et al. (2017). Ozone and haze pollution weakens net primary productivity in China. *Atmospheric Chemistry and Physics*, *17*(9), 6073–6089. https://doi.org/10.5194/acp-17-6073-2017

Zanis, P., Akritidis, D., Turnock, S., Naik, V., Szopa, S., Georgoulias, A. K., et al. (2022). Climate change penalty and benefit on surface ozone: A global perspective based on CMIP6 earth system models. *Environmental Research Letters*, *17*(2), 024014. https://doi.org/10.1088/1748-9326/ac4a34

Zhang, J., & Chen, F. (2022). Future projections of daily maximum and minimum temperatures over East Asia for the carbon neutrality period of 2050-2060. *Theoretical and Applied Climatology*, *150*(1–2), 203–213. https://doi.org/10.1007/s00704-022-04155-9

Zhang, Y., Hu, X.-M., Leung, L. R., & Gustafson, J. W. I. (2008). Impacts of regional climate change on biogenic emissions and air quality. *Journal of Geophysical Research*, *113*(D18), D18310. https://doi.org/10.1029/2008JD009965

Zhang, Y., Zhang, R., Yu, J., Zhang, Z., Yang, W., Zhang, H., et al. (2020). Isoprene mixing ratios measured at twenty sites in China during 2012–2014: Comparison with model simulation. *Journal of Geophysical Research: Atmospheres*, *125*(24), e2020JD033523. https://doi.org/10.1029/2020JD033523

Zhou, Y., Yang, Y., Wang, H., Wang, J., Li, M., Li, H., et al. (2022). Summer ozone pollution in China affected by the intensity of Asian monsoon systems. *Science of the Total Environment*, *849*, 157785. https://doi.org/10.1016/j.scitotenv.2022.157785

References From the Supporting Information

Gelaro, R., McCarty, W., Suárez, M. J., Todling, R., Molod, A., Takacs, L., et al. (2017). The modern-era retrospective analysis for Research and applications, version 2 (MERRA-2). *Journal of Climate*, *30*(14), 5419–5454. https://doi.org/10.1175/JCLI-D-16-0758.1

Park, R. J., Jacob, D. J., Field, B. D., Yantosca, R. M., & Chin, M. (2004). Natural and transboundary pollution influences on sulfate-nitrate-ammonium aerosols in the United States: Implications for policy. *Journal of Geophysical Research*, *109*(D15), D15204. https://doi.org/10.1029/2003jd004473

Pye, H. O. T., Liao, H., Wu, S., Mickley, L. J., Jacob, D. J., Henze, D. K., & Seinfeld, J. H. (2009). Effect of changes in climate and emissions on future sulfate-nitrate-ammonium aerosol levels in the United States. *Journal of Geophysical Research*, *114*(D1), D01205. https://doi.org/10.1029/2008jd010701

Mao, J., Paulot, F., Jacob, D. J., Cohen, R. C., Crounse, J. D., Wennberg, P. O., et al. (2013). Ozone and organic nitrates over the eastern United States: Sensitivity to isoprene chemistry. *Journal of Geophysical Research: Atmospheres*, *118*(19), 11256–11268. https://doi.org/10.1002/jgrd.50817

Bey, I., Jacob, D. J., Yantosca, R. M., Logan, J. A., Field, B. D., Fiore, A. M., et al. (2001). Global modeling of tropospheric chemistry with assimilated meteorology: Model description and evaluation. *Journal of Geophysical Research*, *106*(D19), 23073–23095. https://doi.org/10.1029/2001JD000807

Lin, J.-T., & McElroy, M. B. (2010). Impacts of boundary layer mixing on pollutant vertical profiles in the lower troposphere: Implications to satellite remote sensing. *Atmospheric Environment*, *44*(14), 1726–1739. https://doi.org/10.1016/j.atmosenv.2010.02.009

McLinden, C. A., Olsen, S. C., Hannegan, B., Wild, O., Prather, M. J., & Sundet, J. (2000). Stratospheric ozone in 3-D models: A simple chemistry and the cross-tropopause flux. *Journal of Geophysical Research*, *105*(D11), 14653–14665. https://doi.org/10.1029/2000jd900124

Rodriguez, J. D., Perez, A., & Lozano, J. A. (2010). Sensitivity analysis of k-fold cross validation in prediction error estimation. *IEEE Transactions on Pattern Analysis and Machine Intelligence*, *32*(3), 569–575. https://doi.org/10.1109/TPAMI.2009.187